Aspects of a turbulent-nonturbulent interface

Aspects of a turbulent-nonturbulent interface

V D Narasimhamurthy[1], H I Andersson[1] and B Pettersen[2]

[1] Fluids Engineering Division, Department of Energy and Process Engineering, Norwegian University of Science and Technology (NTNU), NO-7491 Trondheim, Norway
[2] Dept. of Marine Technology, Norwegian University of Science and Technology, NO-7491 Trondheim, Norway

E-mail: vagesh@alumni.ntnu.no

Abstract. Transport mechanisms at the interface between a laminar and a turbulent plane Couette flow are examined by means of DNS data of a statistically steady flow field. A mixing-layer is established which neither evolves in the streamwise direction nor in time. This novel flow configuration is perfectly suited for explorations of momentum transfer mechanisms, e.g. turbulent diffusion. Unexpected undulations characterize the large-scale interactions between the turbulent and the nominally non-turbulent part flow. However, surprisingly large velocity fluctuations are observed even in the low-Re half of the flow which otherwise would be laminar.

1. Introduction

The shear-driven flow of an incompressible and isothermal fluid between two parallel plates in relative motion, popularly termed as turbulent plane Couette flow, is arguably one of the classic non-trivial problems in fluid mechanics. In the present contribution, a modification to this original flow problem is considered, where the (top) moving wall is divided in two equal parts with different velocities as shown in figure 1. The wall velocity ratio $U_1/U_2 = 5$ and the Reynolds numbers (based on half the velocity difference between the moving and stationary wall and the channel half-height h) are $Re_1 = U_1 h/2\nu = 1300$ and $Re_2 = U_2 h/2\nu = 260$. We already know from the literature (see Schneider *et al.* (2010) and Tuckerman & Barkley (2011) for literature review) that the subcritical transition Reynolds number Re_c for plane Couette flow is in between $300 - 370$ and the Reynolds number for establishing fully developed turbulence is $500 - 600$. Thereby, in the present case laminar and turbulent flow regimes co-exist side-by-side. The aim of this novel problem is to understand the mixing behaviour at the turbulent-nonturbulent interface and investigate the entrainment mechanisms.

2. Flow configuration and numerical method

The Navier-Stokes equations for an incompressible and isothermal flow are solved in three-dimensional space and time using a parallel Finite Volume code called MGLET (Manhart, 2004). The code uses staggered Cartesian grid arrangements. Spatial discretization of the convective and diffusive fluxes are carried out using a 2^{nd}-order central-differencing scheme. The momentum equations are advanced in time by a fractional time stepping using a 2^{nd}-order explicit Adams-Bashforth scheme. The Poisson equation for the pressure is solved by a full multi-grid method based on pointwise velocity-pressure iterations. The computational

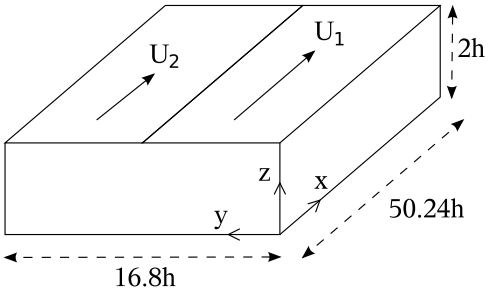

Figure 1. Flow configuration (not to scale). Top wall in two halves moving at different speed.

grid is divided into an arbitrary number of subgrids that are treated as dependent grid blocks in parallel processing. In the present study, the size of the computational domain in each coordinate direction $L_x \times L_y \times L_z$ is $50.24h \times 16.8h \times 2h$, i.e. same as in the turbulent plane Couette flow study of Holstad *et al.* (2006). Aided by their two-point correlation data, Holstad *et al.* (2006) concluded that the present domain size is appropriate for the Reynolds number considered. In this paper we report results of a marginally resolved DNS using $256 \times 256 \times 64$ grid points (see table 1 for grid details). A fully resolved simulation is underway. Uniform grid spacing is adopted in the streamwise and the spanwise directions, while a non-uniform mesh is used in the wall-normal direction. The time-step $\Delta t = 0.05$. Periodic boundary conditions were employed in the streamwise and spanwise directions. No-slip and impermeability conditions were imposed on the walls. The mean velocity field and the turbulence statistics have been deduced by first averaging in time and in the homogeneous streamwise direction. The time-averaging was performed over 4000 statistical sample fields, each separated by 0.1625 h/u_τ.

Table 1. Numerical and flow parameters from various turbulent plane Couette flow studies. In all the cases $Re = 1300$ and the channel height $L_z/h = 2$. Re_τ is the Reynolds number based on the wall-friction velocity u_τ and Δ^+ is the grid resolution in wall-units.

Case	Re_τ	L_x/h	L_y/h	$N_x \times N_y \times N_z$	Δ_x^+	Δ_y^+	Δ_z^+
Bech *et al.* (1995)	82.2	10π	4π	$256 \times 256 \times 70$	10.1	4.0	$0.7 - 3.9$
Hu *et al.* (2003)	82	192	24	$1024 \times 512 \times 81$	15.38	7.69	—
Holstad *et al.* (2006)	84.6	50.24	16.8	$256 \times 256 \times 64$	16.60	5.55	$2.03 - 3.35$
Holstad *et al.* (2010)	82.5	16π	6π	$768 \times 288 \times 192$	5.40	5.40	$0.33 - 1.74$
Present case	84.6	50.24	16.8	$256 \times 256 \times 64$	16.60	5.55	$2.03 - 3.35$

3. Results

3.1. Turbulent flow field

Figure 2(b,d,f) illustrates the velocity fluctuations in the channel mid-plane from the present computations. For comparison, corresponding data from the reference case, i.e. from the present plane turbulent Couette flow case is included in figure 2(a,c,e). The instantaneous flow pattern in figure 2(b,d,f) shows that the flow midway between the fixed and the moving wall is vigorously turbulent over roughly 50% of the width but far from strictly being laminar in the other half, i.e. $y/h > 8$, even though the local Reynolds number Re_2 is below Re_c. The streamwise and wall-normal fluctuations in figure 2(b) and 2(f) together with the alternate bands of positive and negative fluctuations of spanwise velocity in figure 2(d) clearly indicate the meandering motion in the interaction zone between the turbulent and the non-turbulent regimes. It can be

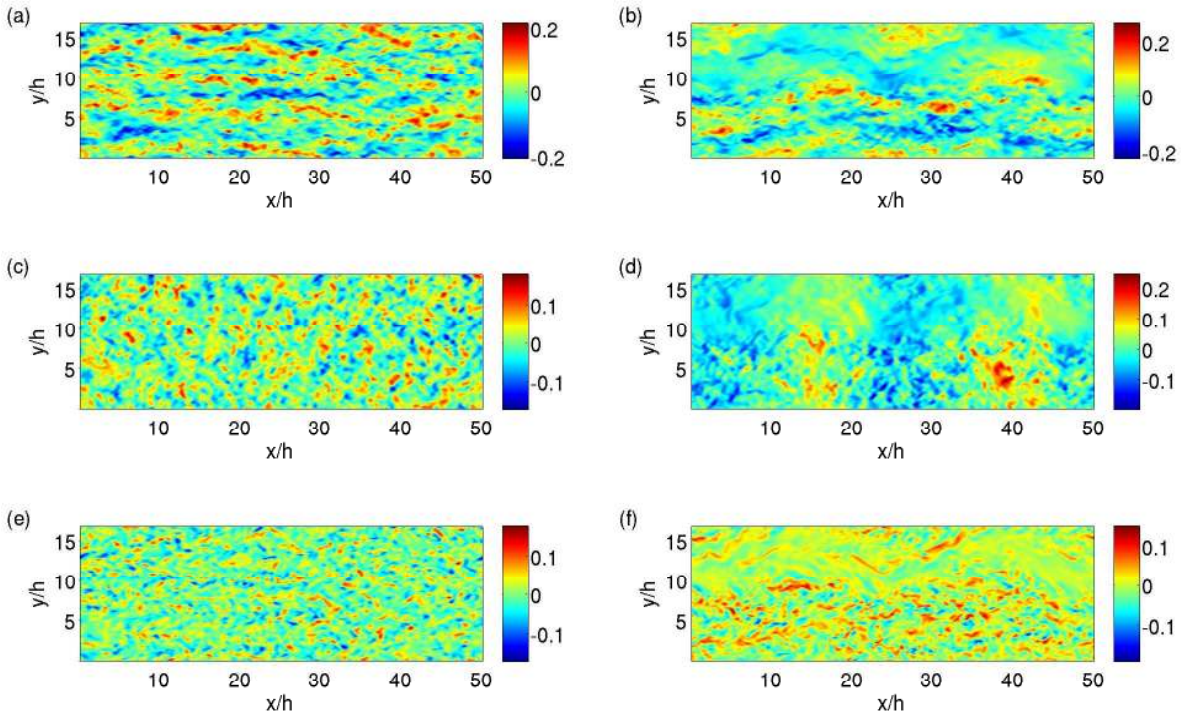

Figure 2. Instantaneous velocity fluctuations in the mid-plane from the present case (b, d, f) compared against the turbulent plane Couette flow data (a, c, e). All contours are normalized by U_1. (a, b) streamwise fluctuation u'; (c, d) spanwise fluctuation v'; (e, f) wall-normal fluctuation w'.

noticed from figure 2(b) that the large-scale streamwise structures, which are typically observed in the core-region of the turbulent plane Couette flow (Komminaho *et al.*, 1996; Papavassiliou & Hanratty, 1997; Tsukahara *et al.*, 2006), persist even in the turbulent part of the present domain, i.e. $y/h < 8$ (for comparison see figure 2(a)).

Contours of streamwise velocity fluctuations in the vicinity of the walls are shown in figure 3. Two distinct flow patterns can be seen in figure 3(a) which indicate that the meandering motion is not established near the (top) moving walls owing to the sudden discontinuity in the local Reynolds number. However, away from the moving walls the interaction between the low and high speed flow eventually causes meandering and these undulations will probably tend to

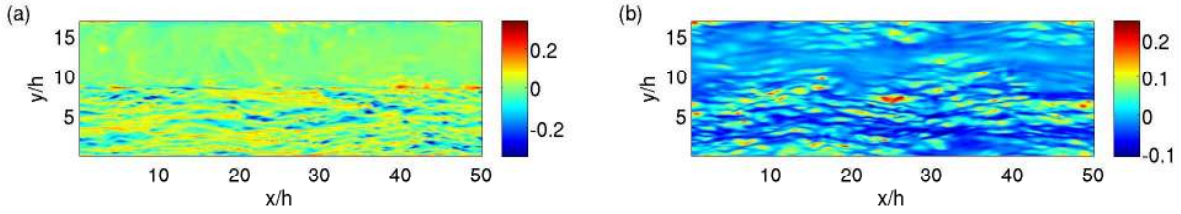

Figure 3. Contours of streamwise velocity fluctuations u'/U_1 in an $xy-$plane at $z^+ = 5$ from (a) the top moving wall and from (b) the bottom fixed wall.

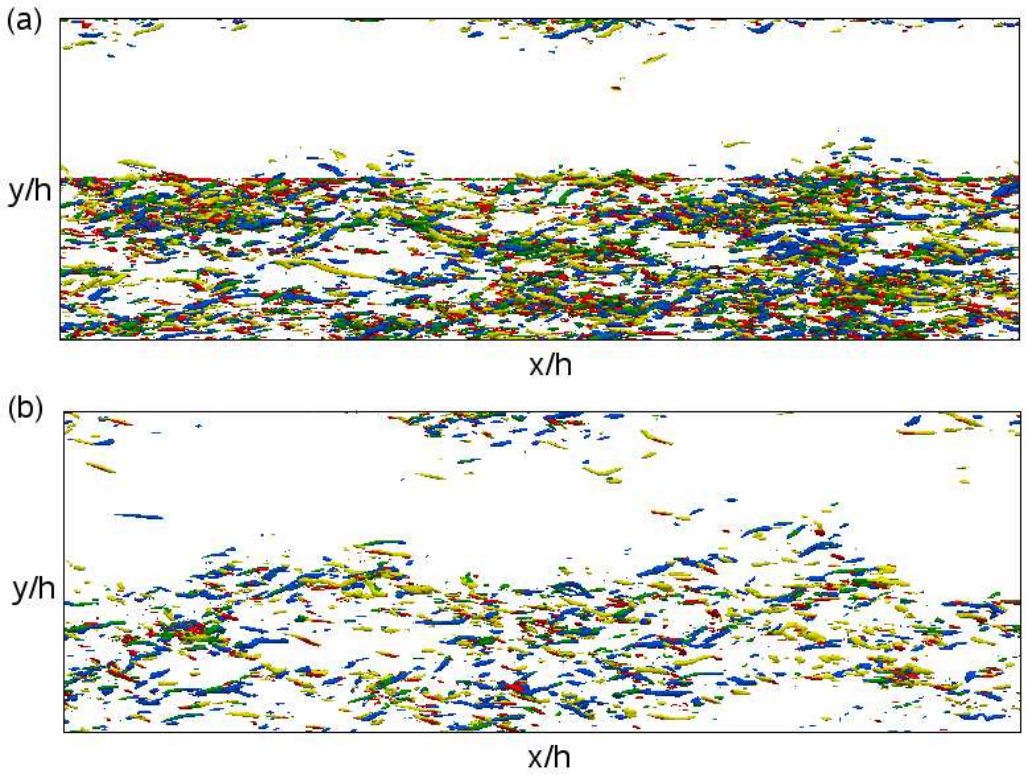

Figure 4. Three-dimensional instantaneous vortical structures in the present case: (a) top half of the domain; (b) bottom half of the domain. Surfaces coloured yellow and blue mark positive and negative values of $\lambda_2\omega_x$ and red and green mark positive and negative values of $\lambda_2\omega_z$, respectively.

enhance the spanwise mixing (cf. figure 2(b) and 3(b)). These features are also well illustrated in figure 4, where iso-surfaces of three-dimensional vortical structures are plotted. In addition to the streamwise vorticity component ω_x, the wall-normal vorticity ω_z was found to be important since it contributes to the mixing in $(x, y)-$planes.

The cross-sectional view of the velocity field in figure 5(b) shows that counter-rotating secondary roll-cells or Taylor-Görtler-like vortices fill the entire cross section in the present case (flow topography from the present turbulent plane Couette flow case is shown in figure 5(a) for comparison). Such roll-cells are well known in numerically simulated turbulent plane Couette flows (Bech *et al.*, 1995; Komminaho *et al.*, 1996; Papavassiliou & Hanratty, 1997; Tsukahara *et al.*, 2006), but have never been observed in a nominally non-turbulent flow. It is conjectured that the roll-cells develop here since the flow in the low-Re half of the channel is turbulent-like rather than laminar as it should have been according to the low local $Re_2 = 260$. The spanwise size of the roll-cells is distinctly different in the two parts of the flow and this suggests that their size is in some way related to the local Re. By means of the data base which will result from the fully resolved simulation, the interfacial mixing processes will be further explored.

3.2. Turbulence statistics

The wall-normal variation of the mean streamwise velocity selected at some equi-distant positions along the span y/h are shown in figure 6. Note that the data from the present turbulent plane Couette flow case is in excellent agreement with DNS data from Bech *et al.* (1995). On the contrary in the present case at $y/h = 4.2$, i.e. in the middle of the $Re_1 = 1300$ region,

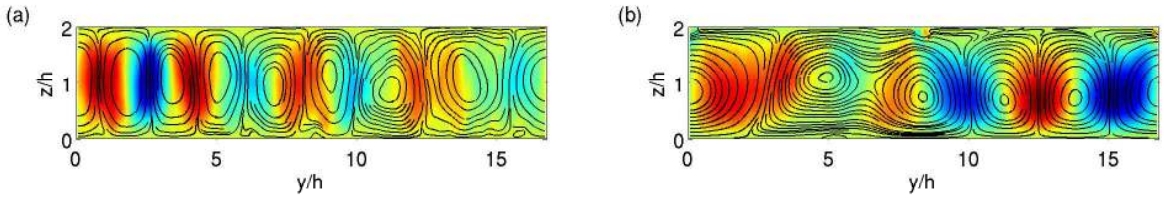

Figure 5. Mean secondary flow streamlines in the $yz-$plane together with the wall-normal velocity contours in the background: (a) turbulent plane Couette flow; (b) present case (note that $y/h = 0 - 8.4$ corresponds to the turbulent zone and $y/h = 8.4 - 16.8$ corresponds to laminar regime).

the magnitude of the U velocity has drastically reduced and the conventional anti-symmetric variation of the mean velocity profile is broken when compared to the turbulent plane Couette flow data. On the other hand, the U velocity at $y/h = 12.6$ surprisingly exhibits a parabolic like profile. This is especially striking, since at the centre of the $Re_2 = 260$ region the flow is expected to be laminar and the velocity profile should therefore have been linear.

Variation of the root-mean-square values of the fluctuating velocities and the turbulent shear stress from the present case are compared against the benchmark turbulent plane Couette flow data in figure 7. In general, the conventional symmetry of all the profiles is broken. The velocity fluctuations in the streamwise and wall-normal direction shown in figure 7(a) and 7(c), respectively, are close to the DNS data of Bech *et al.* (1995) at $y/h = 4.2$. In contrast, the spanwise fluctuations v_{rms} is highly enhanced in the present case when compared to Bech *et al.* (1995) (see figure 7(b)). On the other hand, u_{rms}, v_{rms} and w_{rms} attain appreciable levels also in the centre of the $Re_2 = 260$ region ($y/h = 12.6$) where the flow should be laminar. Here, turbulence intensities of about 50% of those in the fully turbulent half of the flow are observed. Note that w_{rms} is the least-affected component when compared to the other two since this component is perpendicular to the plane of mixing. The present turbulent shear stress data at $y/h = 4.2$ in figure 7(d) varies along the wall-normal direction in the core-region $z/h = 0.5 - 1.5$ contrary to the constant shear stress profile of Bech *et al.* (1995). On the other hand, the profile at $y/h = 12.6$ becomes slightly negative near the moving wall, i.e. around $z/h = 1.7$. All these unexpected observations will be further explored and interpreted on the basis of data from the refined DNS. In particular, the thickness of the turbulent/nonturbulent interface will be deduced

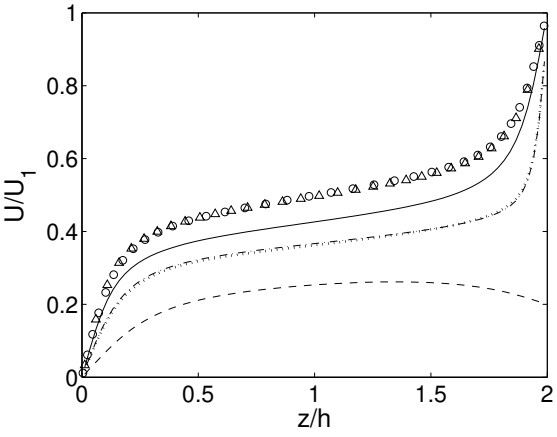

Figure 6. Wall-normal distribution of mean streamwise velocity from the present case at various spanwise positions: $\cdots\cdots, y/h = 0$; ——, $y/h = 4.2$; — · —, $y/h = 8.4$; - - - -, $y/h = 12.6$; and the corresponding data from the present turbulent plane Couette flow case (△) compared with the DNS data of Bech *et al.* (1995) (○).

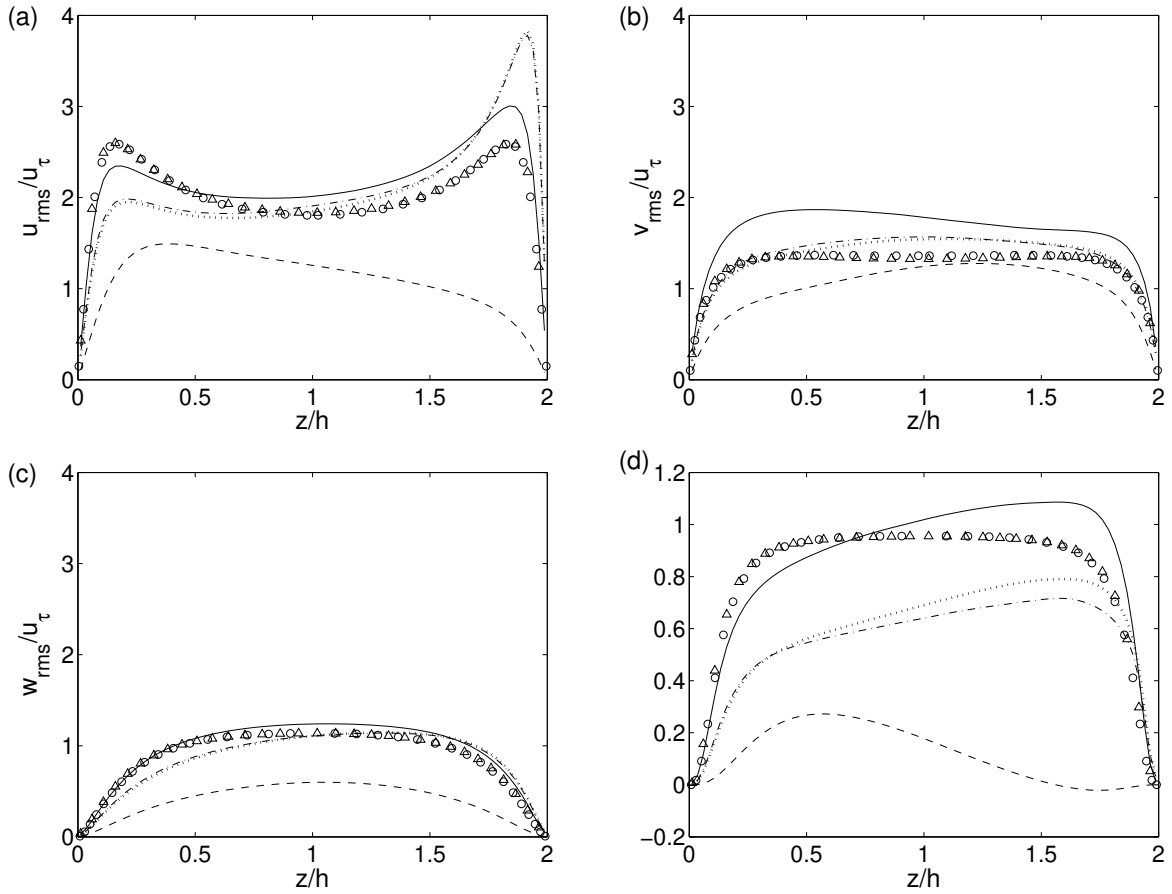

Figure 7. Wall-normal distribution of turbulence intensities: (a) u_{rms}/u_τ; (b) v_{rms}/u_τ; (c) w_{rms}/u_τ; and the turbulent shear stress (d) $-\rho\overline{uw}/\tau_w$ from the present case at various spanwise positions (see figure 6 for legend).

similarly as in Da Silva & Taveira (2010).

4. Conclusion

Contrary to the classical mixing-layer, a new mixing-layer is established which neither evolves in the streamwise direction nor in time but instead varies perpendicular to the plane of mixing. This new mixing-layer is realizable in the junction between two co-current plane Couette flows. The interaction between the low- and high-speed flow regimes is characterized by large-scale undulations, which tends to enhance the mixing between the turbulent and the nominally non-turbulent part flow.

Acknowledgments

The authors express gratitude to the financial support from Research Council of Norway through the KMB project "Investigating Hydrodynamic Aspects and Control Strategies for Ship-to-Ship Operations" at MARINTEK.

References

Bech, K. H., Tillmark, N., Alfredsson, P. H. & Andersson, H. I. 1995 An investigation of turbulent plane Couette flow at low Reynolds numbers. *J. Fluid Mech.* **286**, 291–325.

Da Silva, C. B. & Taveira, R. R. 2010 The thickness of the turbulent/nonturbulent interface is equal to the radius of the large vorticity structures near the edge of the shear layer. *Phys. Fluids* **22**, 121702.

Holstad, A., Andersson, H. I. & Pettersen, B. 2010 Turbulence in a three-dimensional wall-bounded shear flow. *Int. J. Numer. Methods Fluids* **62**, 875–905.

Holstad, A., Johansson, P. S., Andersson, H. I. & Pettersen, B. 2006 On the influence of domain size on POD modes in turbulent plane Couette flow. In *Proc. of the 6th Int. ERCOFTAC Workshop on Direct and Large-Eddy Simulation* (ed. E. Lamballais et al.), *ERCOFTAC Series*, vol. 10, pp. 763–770. Springer.

Hu, Z., Morfey, C. L. & Sandham, N. D. 2003 Sound radiation in turbulent channel flows. *J. Fluid Mech.* **475**, 269–302.

Komminaho, J., Lundbladh, A. & Johansson, A. V. 1996 Very large structures in plane turbulent Couette flow. *J. Fluid Mech.* **320**, 259–285.

Manhart, M. 2004 A zonal grid algorithm for DNS of turbulent boundary layers. *Comput. Fluids* **33**, 435–461.

Papavassiliou, D. V. & Hanratty, T. J. 1997 Interpretation of large-scale structures observed in a turbulent plane Couette flow. *Int. J. Heat and Fluid Flow* **18**, 55–69.

Schneider, T. M., Lillo, F. D., Buehrle, J., Eckhardt, B., Dörnemann, T., Dörnemann, K. & Freisleben, B. 2010 Transient turbulence in plane Couette flow. *Phys. Rev. E* **81**, 015301.

Tsukahara, T., Kawamura, H. & Shingai, K. 2006 DNS of turbulent Couette flow with emphasis on the large-scale structure in the core region. *J. Turbul.* **7**, N 19.

Tuckerman, L. S. & Barkley, D. 2011 Patterns and dynamics in transitional plane Couette flow. *Phys. Fluids* **23**, 041301.